RSC Advances

PAPER

View Article Online
View Journal | View Issue

Cite this: *RSC Adv.*, 2016, **6**, 104131

A room temperature hydrogen sulfide gas sensor based on electrospun polyaniline–polyethylene oxide nanofibers directly written on flexible substrates†

Saeb Mousavi,[ab] Kyungnam Kang,[ab] Jaeho Park[ab] and Inkyu Park*[ab]

Received 17th August 2016
Accepted 24th October 2016

DOI: 10.1039/c6ra20710c

www.rsc.org/advances

A flexible hydrogen sulfide (H_2S) gas sensor based on polyaniline–polyethylene oxide (PAni–PEO) nanofibers doped by camphorsulfonic acid (HCSA) is presented in this paper. The proposed sensor exhibits good sensitivity, good recovery speed and superior performance compared with previously proposed H_2S PAni-based sensors. The sensor was fabricated by a simple and low-cost procedure on flexible paper and polyimide substrates. Substrates with pre-fabricated metal electrodes were placed in front of the syringe needle of the electrospinning setup and electrospun nanofibers were deposited directly on the interdigitated electrodes. The effects of several processing and environmental parameters on the morphology of the nanofibers and their sensitivity to H_2S have been investigated. The cross-sensitivity of the sensor to nitrogen dioxide and acetone, as two interfering gases, has been explored and the sensor showed good selectivity towards H_2S. The proposed sensor can be used in wearable applications and has the potential to be used in a number of applications such as in industrial plants, and in monitoring human body/mouth odor and foods' freshness.

Introduction

Detecting ultra-low levels of toxic chemicals is increasingly important in personal and industrial applications. One of these hazardous chemicals is hydrogen sulfide (H_2S), which desensitizes the olfactory senses preventing the detection of its distinctive rotten egg smell at high concentrations.[1,2] According to the NIOSH (National Institute for Occupational Safety and Health), the IDLH (immediately dangerous to life or health concentration) for H_2S is 100 ppm. Exposure should not exceed 20 ppm with the following exception: if no other measurable exposure occurs during the 8 hour work shift, exposures may exceed 20 ppm, but not more than 50 ppm, for a single time period up to 10 minutes.[3] So far, several sensors with different working principles, either at room temperature or high temperature, have been proposed for the detection of this gas at low concentrations.[4–11] Polyaniline (PAni) is a conducting polymer which has a uniquely simple doping/de-doping chemistry based on the acid/base reactions. When the blue non-conducting emeraldine base comes into contact with an acidic vapor, it rapidly dopes to form a green conducting emeraldine salt. This change is seen as a dramatic decrease in the electrical resistance.[1] Conventional PAni sensors were synthesized either as a thin film or in the form of nanofibers. Although thin film PAni based sensors have been investigated as low cost and versatile gas sensors for a variety of toxic gases including H_2S, a PAni-based sensor with good response and recovery time for H_2S gas has not been proposed before.[12–17] PAni nanofiber (NF) sensors showed higher performance as compared with the thin film sensors.[1,18] When PAni has a nanofibrillar morphology, the resistance change is more than 10 times faster than that of a conventional PAni thin film.[1] This higher performance is due to the higher surface to volume ratio of nanofibers that provides larger reaction sites and therefore increases the sensitivity and shortens the recovery time. Electrospinning is a simple and efficient method for synthesizing PAni NFs and it has been employed for synthesizing PAni NFs previously.[12,13] PAni NF gas sensors showed high sensitivity and rapid recovery to low concentrations of target gases such as nitrogen dioxide and ammonia.[12] However, to the best of our knowledge, nobody have reported thus far a PAni NF sensor for the detection of low concentrations (1 to 20 ppm) of H_2S gas with acceptable performance (*i.e.* appropriate response and recovery). Previous sensors based on PAni thin films showed good sensitivity to relatively high concentrations (>20 ppm) of H_2S gas, but they showed no or very poor recovery.[14,19,20] On contrary, our sensor shows almost full recovery after the exposure to different concentrations of H_2S gas and it also shows

[a]*Department of Mechanical Engineering, Korea Advanced Institute of Science and Technology (KAIST), Daejeon 305-701, Korea. E-mail: inkyu@kaist.ac.kr*

[b]*KAIST Institute for the Nanocentury (KINC), Korea Advanced Institute of Science and Technology (KAIST), Daejeon 305-701, Korea*

† Electronic supplementary information (ESI) available. See DOI: 10.1039/c6ra20710c

good stability. To explore the cross-sensitivity of the sensor to other gases, two other gases have been also targeted, acetone, which is a source of halitosis like H_2S, and nitrogen dioxide (NO_2), which is a common environmental pollutant like H_2S.

Results and discussion

Morphology of electrospun nanofibers

Physical and chemical characteristics of nanofibers are characterized in this section. Several parameters can affect the physical structure of PAni NFs. Here we investigate the effect of molecular weight of PAni, concentration of the binder, polyethylene oxide (PEO), relative humidity (RH) of ambient and successful solution filtration on the morphology of nanofibers. In order to obtain high quality nanofibers, *i.e.* long nanofibers with lowest level of agglomerates and beads and with reasonable base resistance, electrospinning was done with several different solutions.

The presence of polymeric binder is an important parameter when synthesizing the nanofibers. The PEO as binder in solution increases the solution viscosity and helps the formation of continuous nanofibers web. The viscosities of electrospinning solutions with different concentrations of PEO (1, 3 and 6%) were measured by a SV-10 VIBRO Viscometer. The solutions with 1, 3 and 6% PEO dissolved showed 3.4, 20.5 and 82.7 mPa s of viscosity, respectively, at 23 °C. It is clear from these results that adding PEO directly increases the viscosity of solution. According to our experiments, formation of nanofibers web is not possible without sufficient amount of binder in the electrospinning solution. On the other hand, high concentration of PEO results in the formation of thicker fibers and in some parts causes fibers to stick to the neighboring fiber (please see Fig. 1(c)). This clearly reduces the surface to volume ratio and as a result the surface area available for the reaction with gas molecules. Fig. 1(a)–(c) show how increasing the binder concentration can help the formation of nanofibers web. The molecular weight of polymers is another important synthesis parameter. According to our experiments, formation of smooth or beady nanofibers can be determined by changing the molecular weight of the polymeric components. Fig. 1(d) and (e) show how increasing the molecular weight of PAni can help the formation of nanofibers with less beads. Higher molecular weight results in higher viscosity and less beads, which showed higher conductivity. These fibers have been synthesized with similar parameters and they are only different in PAni molecular weight. Two used molecular weights are 65 000 and 10 000. The nanofibers obtained with higher molecular weight (65k) show 1.2 MΩ resistance in ambient air, but the nanofibers obtained with lower molecular weight (10k) show 70 MΩ resistance in the same environment.

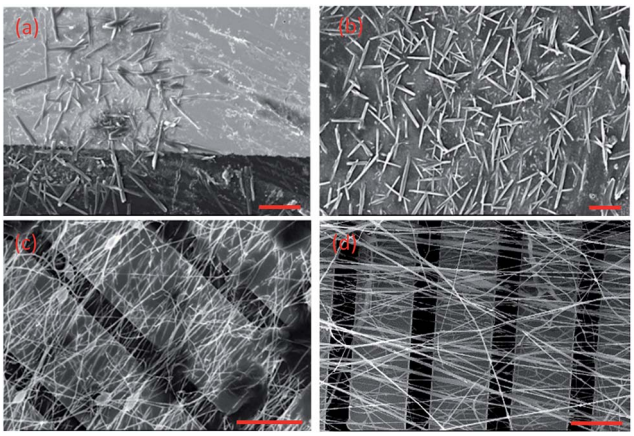

Fig. 2 Effect of humidity on the formation of nanofibers web. SEM images of nanofibers electrospun with the same parameters but in different relative humidities: (a) 70%, (b) 65%, (c) 50% and (d) 30%. The scale bars are 20 μm in (a) and (b) and 10 μm in (c) and (d).

Since the humidity is a very important parameter when synthesizing the nanofibers, we investigated the effect of humidity on the morphology of the nanofibers. Low humidity may increase the velocity of the solvent evaporation. On the contrary, high humidity will lead to the thick fiber diameter owing to the charges on the jet can be neutralized and the stretching forces become small.[21] While maintaining all the other parameters the same, we synthesized PAni–PEO NFs in

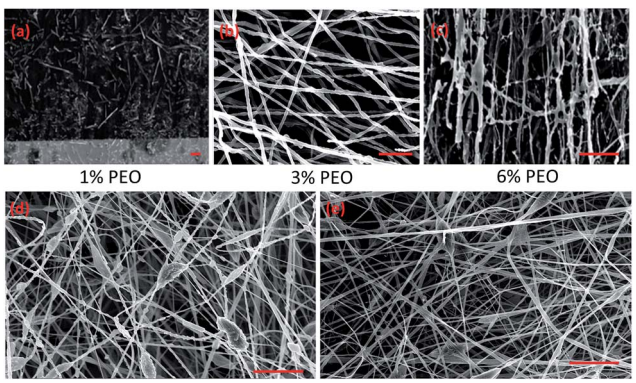

Fig. 1 Effect of binder concentration on the formation of nanofibers web (a–c). (d) Formation of beady nanofibers (PAni 10k–PEO) *versus* (e) less beady PAni 65k–PEO nanofibers. The scale bars are 5 μm in (b) and (c), and 10 μm in (a), (d) and (e).

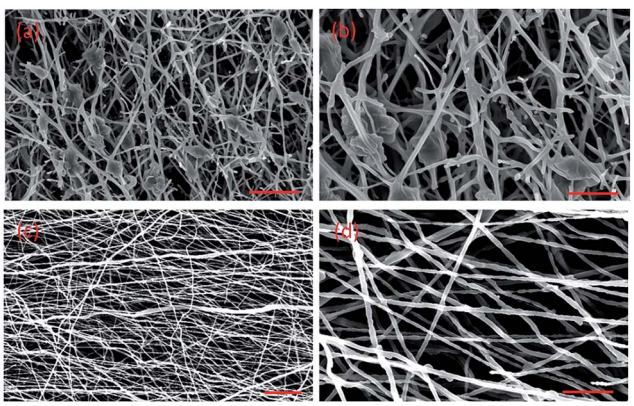

Fig. 3 Effect of solution filtration on the formation of nanofiber web: (a) and (b) nanofibers obtained from un-filtered solution; (c) and (d) nanofibers obtained from filtered solution. The scale bars are 5 μm in (b) and (d), and 10 μm in (a) and (c).

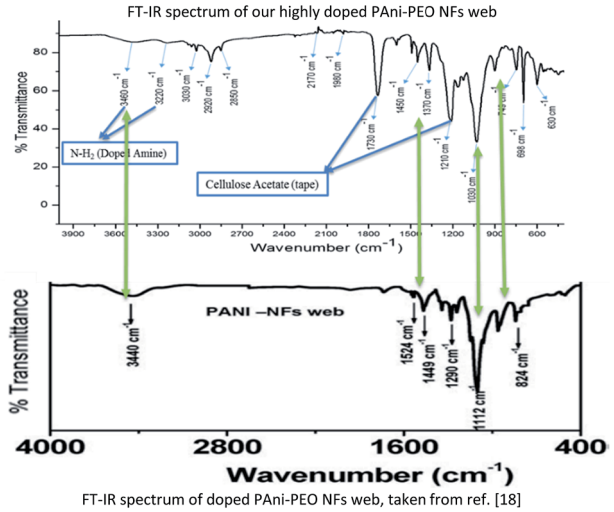

FT-IR spectrum of doped PAni-PEO NFs web, taken from ref. [18]

Fig. 4 Matching FTIR spectrum of doped PAni–PEO nanofibers synthesized on a 3 M (cellulose acetate) tape substrate with a previously proposed spectrum in ref. 22.

four different relative humidity (RH) conditions, 75%, 65%, 50% and 30%. It is clearly observed that in the conditions with the RH equal to or higher than 65%, no continuous thin nanofibers could be formed and only thicker and short fibers could be formed. On the other hand, under RH of 50% and 30%, long and continuous nanofibers were formed as shown in Fig. 2.

The electrospinning solution was filtered using a PTFE syringe filter (pore size = 0.45 μm). Successful filtration is very important in the formation of nanofiber web with acceptable resistance and sensitivity. As shown in Fig. 3, when filtration was not successfully done, agglomerates exist in the synthesized web, which dramatically increases the resistance of the web. These agglomerates, which were not filtered, contain undissolved PAni EB and act as insulating junctions. The doping process of PAni EB occurs inside the solvent and the bigger undissolved particles will not be doped by HCSA. As a result, these agglomerates have very high resistances and act like electron barriers inside the web of nanofibers. These electron barriers will block the majority of electrons that are able to move on doped PAni's chains and therefore significantly increase the resistance of the nanofibers. The measured resistance for the nanofibers on the interdigitated sensor electrodes was ~1 MΩ in case of successful filtration, but it was larger than 10 GΩ for the nanofibers obtained from the unfiltered solution.

To characterize the chemical structure of nanofibers and determine the existing functional groups, Fourier transform infrared (FTIR) spectroscopy was employed. FTIR spectroscopy was conducted on the electrospun nanofibers deposited on a cellulose acetate tape, with the results shown in Fig. 4. The main characteristic bands of PAni in accordance with those reported in the literature are assigned as follows:[22] two broad bands at 3460 and 3420 cm^{-1} are due to the N–H2 stretching mode, which resulted from the high doping level, the C=N and C=C stretching modes for the quinoid and benzoid rings occur

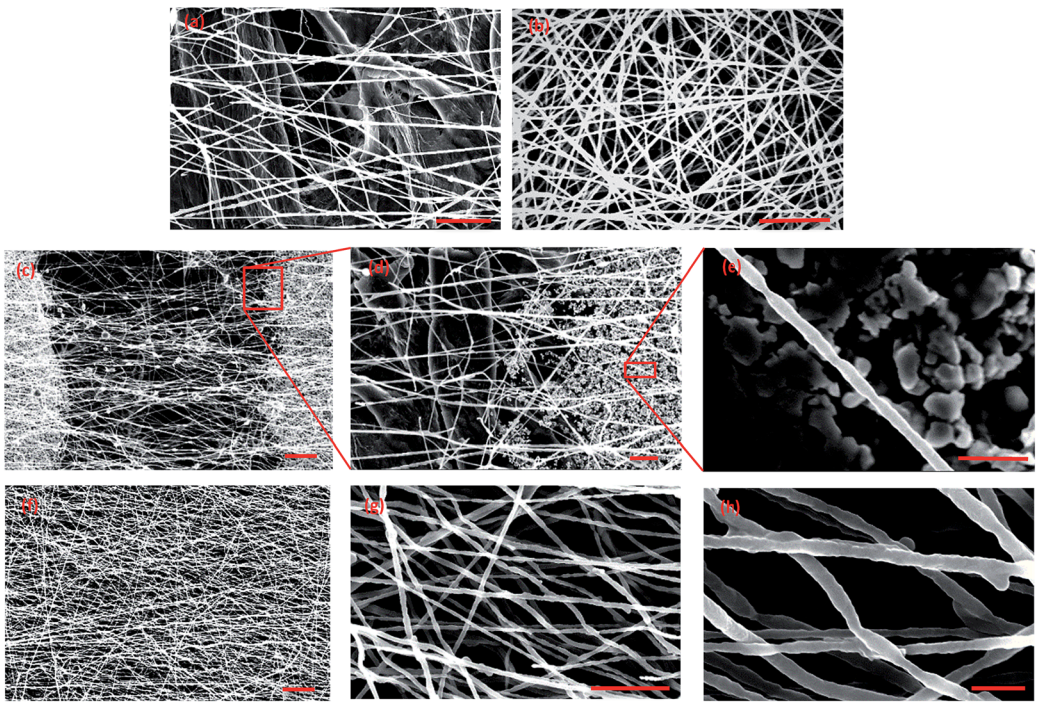

Fig. 5 SEM images of nanofibers deposited on paper substrate for (a) 3 minutes and (b) 5 minutes; (c)–(e) SEM images of the PAni–PEO nanofibers deposited for 3 minutes between two neighboring electrodes on the paper substrate. (f)–(h) SEM images of the PAni–PEO nanofibers deposited for 5 minutes on polyimide (PI) substrate (the scale bars are 10 μm in (a) and (b), 20 μm in (c) and (f), 5 μm in (d) and (g) and 1 μm in (e) and (h)).

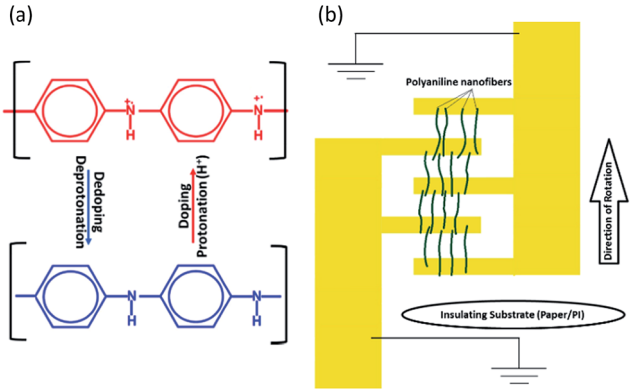

Fig. 6 (a) The doping and dedoping process of PAni molecular chain. (b) PAni NFs, charged on surface, tend to attach to the grounded conductive electrodes and discharge their electrical charges, therefore the nanofibers will be aligned in parallel to each other and perpendicular to the two neighboring electrodes. Direction of the rotation of the substrate (cylinder) improves this alignment.

at 1500 and 1450 cm^{-1}, respectively. The bands at 1990, 1100, and 749 cm^{-1} assigned to the C–N stretching of the secondary aromatic amine, in plane C–H bending and out of plane C–H bending vibration, respectively. The bands at 1450, 1210 and 1030 cm^{-1}, corresponding to the stretching modes of C=N, C=C, and C–N, are shifted to lower wave numbers, which may be attributed to the presence of PEO in the PAni matrix.

Considering the effect of all the environmental and processing parameters mentioned before, on the morphology of the nanofibers, we could synthesize the optimized nanofibers, which are high quality, doped PAni–PEO nanofibers aligned on the electrodes. The synthesized nanofibers were aligned in parallel between two neighboring electrodes, which can greatly decrease the resistance of the sensor. This alignment could be obtained by placing the sensor in the correct direction (*i.e.* parallel electrodes in a perpendicular direction to the direction of rotation) in front of the needle. Since there is an electrical potential between the needle and the conductive electrodes, the nanofibers tend to be attached to the grounded surface of these electrodes, which themselves are located on insulator paper/PI substrates, and discharge their electrical charges. Therefore the nanofibers place in parallel to each other and perpendicular to the two neighboring electrodes (please see Fig. 6(b) and 5(c)).

Fig. 5 shows the optimized nanofibers obtained on the paper and polyimide substrates with different deposition periods (3 and 5 minutes). The average and standard deviation of the nanofibers' diameter, deposited for 3 minutes on the paper substrate were 382 and 101 nm, respectively. For the nanofibers deposited for 3 minutes on the polyimide substrate, the average and standard deviation of the diameter were 293 and 83 nm, respectively. It has been observed that increasing the deposition time from 3 to 5 minutes does not change the diameter of the nanofibers but changing the substrate from PI to paper increases the diameter of the deposited nanofibers. Furthermore, nanofibers' diameter has a wider range and a bigger standard deviation on the paper substrate. This indicates that nanofibers deposited on the PI substrate are more uniform compared with the ones deposited on the paper substrate. Detailed statistical analysis of nanofibers diameter distribution has been performed and can be found in Fig S6 and S7 (ESI†).

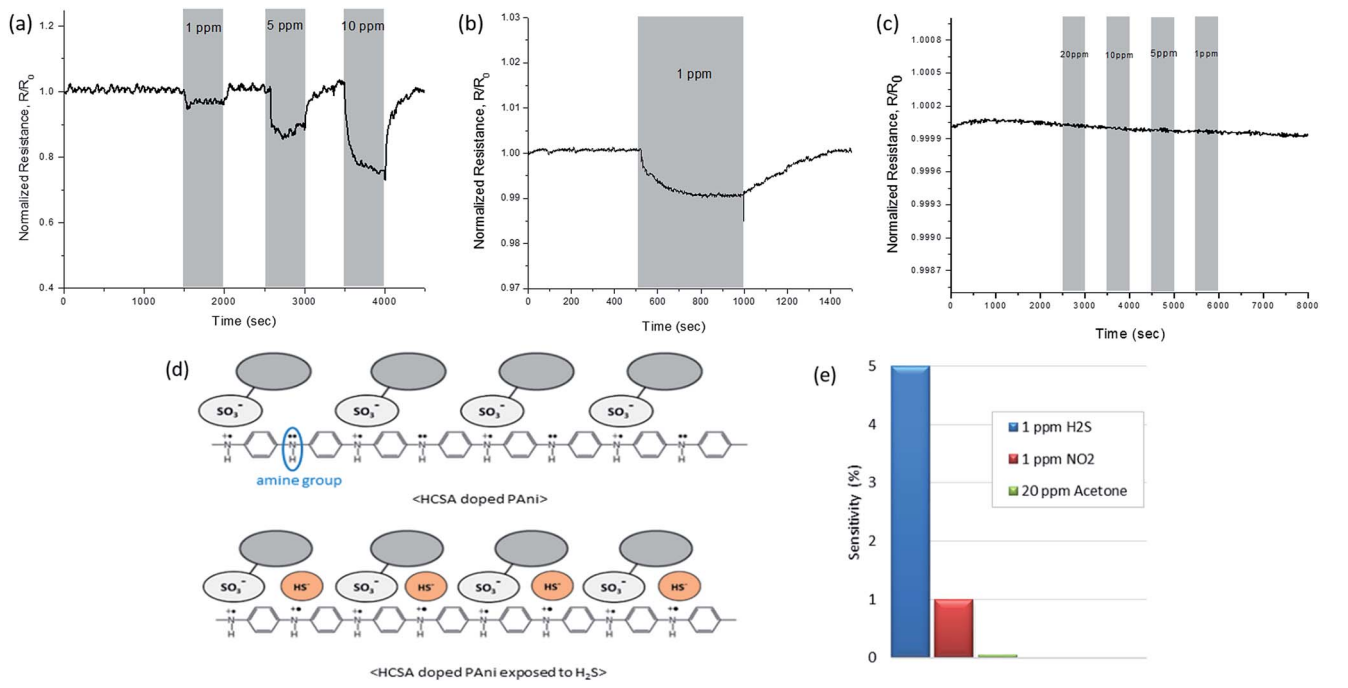

Fig. 7 Responses of PANI–PEO nanofiber based sensor in dry condition to (a) H_2S, (b) NO_2 and (c) acetone gases (d) Sensing mechanism of H_2S gas. H_2S is a protonating gas and further dopes PAni chain. As a result, the resistance of the nanofibers decreases when they are exposed to H_2S gas. (e) Sensor's selectivity toward H_2S; sensitivity of the sensor to 1 ppm H_2S, NO_2 and acetone.

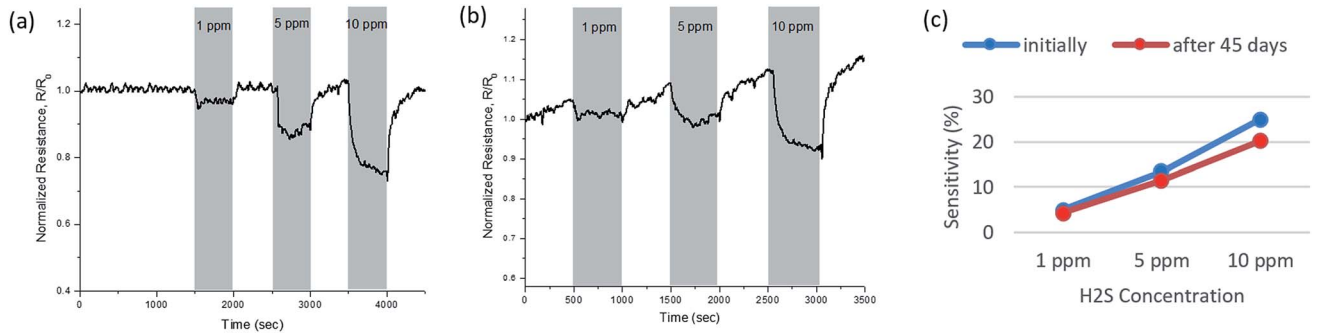

Fig. 8 Stability of PAni–PEO NFs; checking sensor's response to H_2S (a) initially and (b) after 45 days. (c) Comparing the sensor's response to H_2S gas, initially and after 45 days.

Gas sensing results and discussion

Gas sensing tests have been done with sensors based on doped PAni–PEO nanofibers fabricated both on paper and PI substrates. Since we obtained similar results with both of these sensors, we only show the results for the sensors fabricated on the paper substrate in the following. Dynamic responses of the sensor to different gases in dry environment are shown in Fig. 7. For H_2S, the sensor's response and recovery times are 120 and 250 seconds in average, respectively. Also, it shows the responses of $(\Delta R/R_0) \times 100$ (%) = 5%, 13.5% and 25% to 1, 5 and 10 ppm of H_2S gas, respectively.

PAni is a type of conjugated polymer, which are organic macromolecules consisting at least of one backbone chain of alternating double- and single-bonds[23] (shown with a circle in Fig. 6(a)). PAni can be easily doped in an acidic solution (*e.g.* HCl or HCSA solution) or dedoped in a basic solution (*e.g.* aqueous ammonia solution). The doping and dedoping process of PAni is shown in Fig. 6(a). H_2S gas sensing mechanism can be explained as follows: doped PAni is a p-type semiconductor and therefore its major charge carriers are holes. When PAni interacts with H_2S, the following reaction occurs:

$$H_2S + PAni \leftrightarrow HS^- + PAniH^+$$

where $PAniH^+$ indicates the protonated/doped PAni. Since H_2S is an acid, it further dopes PAni, which was already doped by HCSA, by borrowing an electron from the nitrogen in the amine group (see Fig. 7(d)). This will increase the concentration of holes in the PAni chain and enhance the conductivity of PAni NFs.

Besides H_2S, two other gases that often co-exist with H_2S, in different places, nitrogen dioxide (NO_2) and acetone (CH_3-$COCH_3$) have been selected as the interfering gases. Acetone co-exists with H_2S in the smell generated from the rotten food, and also the malodor produced in the human's mouth in case of halitosis. NO_2 is a pollutant that co-exists with H_2S in environmental pollutions, (*e.g.* exhaust gas in industrial plants).

As we conducted a selectivity test against NO_2 and acetone, we could find that the sensor is much less responsive to those gases. As shown in Fig. 7(b and c), the sensor showed only 1% response to 1 ppm of NO_2 gas and no response to acetone. Since NO_2, is an oxidizing gas and doped PAni is a p-type semiconductor, the resistance of doped PAni NFs should decrease when exposed to NO_2, agreeing with the experimental result. Acetone is far less acidic than water (the acid dissociation constant, pK_a for acetone is ~20, while for water it is ~14 and for H_2S it is ~7). The main interaction of acetone with PAni, if any, has to be physical interaction (*e.g.* swelling).[24] Wang, *et al.*[25] demonstrated that acetone swelling into the PAni NFs is negligible in air, which is also approved by our experiments. According to CDC (Center for Disease Control and Prevention), acetone can cause a burning sensation of the eye at a vapor concentration of 500 ppm and the exposure limit is between 1000 and 1500 ppm.[26] According to NIOSH (National Institute for Occupational Safety and Health), NO_2 has an exposure limit of 1 ppm and this value is 50 ppm for H_2S.[1,27] Considering the three types of gases that we targeted, our sensor shows good selectivity toward hydrogen sulfide. The sensitivity of our sensor to 1 ppm of H_2S, 1 ppm of NO_2 and 20 ppm of acetone is compared in Fig. 8(c).

Short-term and long-term stability of the sensor

In order to check the short-term stability and drifting of the fabricated sensor based on electrospun nanofibers, a constant voltage (2 V) was applied and the resistance of the sensor over time was recorded and is shown in Fig. S5 (ESI†). To check the sensor's stability over a long period, the sensor was kept in a low pressure cylinder (away from humidity) for 45 days and its response was tested towards H_2S gas after this period. The result shows 0.7, 2 and 4.7 percent decrease in the sensor's sensitivity to 1, 5 and 10 ppm of H_2S gas, respectively. Also, a small drifting was observed in the sensor's dynamic response. Fig. 8(a and b) illustrates the response of our paper sensor to 10 ppm H_2S, initially and after 45 days.

Humidity dependence

Relative humidity (RH) is one of the most important influencing factors not only during nanofibers' synthesis, but also for the sensor performance. The humidity dependence was tested as compared to H_2S gas in two different RH level (35% and 70%). The humidity was controlled in the gas sensor chamber through a simple method. A saturated salty water was constantly bubbled (by a constant low flow rate of air being injected into

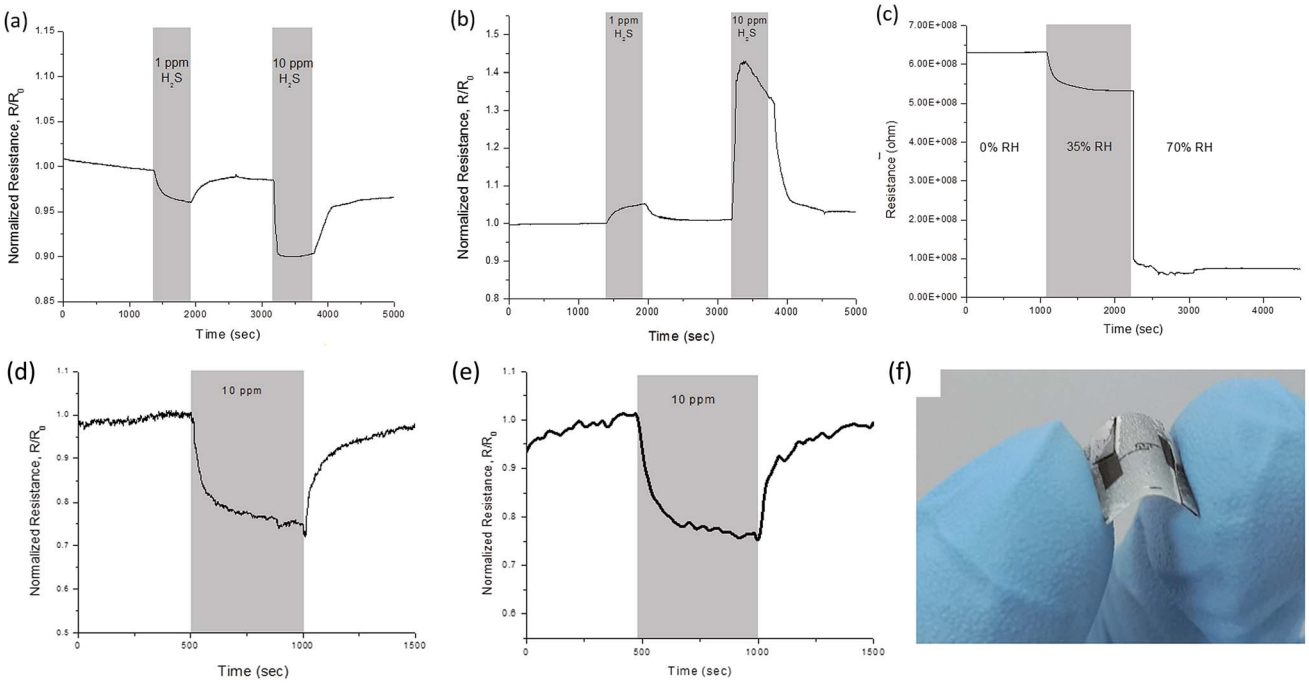

Fig. 9 Effect of RH on the sensor's response. Sensor's response to H_2S in environments with (a) 35% and (b) 70% RH. (c) Base resistance of the sensor drops abruptly by increasing the humidity level. Sensor's response to 10 ppm H_2S in dry air (d) before and (e) after 1000 cycles of mechanical bending test. (f) The photo of a paper sensor in a bent state.

the salty water) to produce water vapor. This water vapor is then mixed with other gases inside the gas chamber. The different RHs have been calibrated simply by using an industrial humidity sensor inside the gas chamber and recording the RH of the chamber for different flow rates of incoming water vapor. It has been observed that the sensor's response is strongly dependent on the ambient RH. The sensor shows 3.5% and 9% sensitivity in 35% RH and 6% and 40% sensitivity in 70% RH to 1 and 5 ppm H_2S, respectively. In highly humid environment (70% RH), there is a debate on why the resistance increases instead of decreasing. Simultaneous mechanisms of different interactions can occur when water vapours are absorbed in the PAni NF as swelling, acid-doping solvation, hydrogen bonding, electron withdrawing, physical entrapment due to the high porosity and roughness, *etc.*[12] In our experiments, it was observed that immediately after increasing the humidity inside the chamber, the resistance of the NFs was dropped by a great degree (please see Fig. 9(c)). The base resistance of nanofibers was around 6.3, 5.4 and 0.8 MΩ in 0%, 35% and 70% RH, respectively. A possible explanation for the sensor's behavior in high RH is brought in the following. Since the water molecules are polar and can act as a weak acid, they can dope PAni NFs, and decrease the resistance of the NFs as a result. Therefore, as the RH increases, the sensitivity of the nanofibers to H_2S decreases. In 35% RH, the nanofibers are already doped by water vapor to some degrees and therefore their response to further doping by H_2S is lower (see Fig. 9(a)). It should be noted that there is a limit for doping PAni NFs. When all the amine groups are doped, further doping is not possible. When RH is very high such as 75%, the PAni molecules are highly doped and H_2S molecules interact with H_2O molecules instead of PAni since no more room exists for further doping in the PAni. H_2S molecules may attract the water molecules on the surface of PAni and form a weak bonding (H_2S–H_2O) since both H_2S and H_2O are polar molecules. Attracting water molecules from the surface of PAni deprotonates it and therefore the resistance increases. When H_2S no longer exists, the humidity on the surface of the PAni chain returns to its previous level, and thus the resistance decreases abruptly again.

Experimental section

Materials

Polyaniline emeraldine base (PAni EB, MW = 65 000), camphorsulfonic acid-β (HCSA), polyethylene oxide (molecular weight = 100 000), chloroform ($CHCl_3$), and tetrahydrofuran (THF) were purchased from Sigma-Aldrich and used without any further purification. Conductive carbon graphite ink (typical resistivity = 48.7 ohms per square) was purchased from Gwent Group. Thermoplastic polyimide (POLYZEN 250T) was purchased from PICOMAX Co., LTD and Whatman® filter paper (pore size ~20 μm) was purchased from Sigma-Aldrich.

Fabrication of sensor substrates and electrodes

Two types of substrates were utilized: filter paper and polyimide (PI) substrate. Conductive carbon microelectrodes were fabricated on a filter paper by a GP-screen printing machine (2030FV, Daeyoung Tech). Conductive carbon paste (C2070424P2 (Gwent group)) screen printed on paper was then

baked in 80 °C oven for 20 minutes. Polyimide (PI) film with a thickness of 15 μm was fabricated by spin coating of liquid PI on silicon handling wafer and subsequent two-step baking process, for 30 minutes at 150 °C and for 4 hours at 250 °C in a convection oven. Then, interdigitated gold microelectrodes were fabricated on PI film by e-beam evaporation and lift-off process. The optical images of patterned substrates are shown in Fig. 10(a)–(f).

Synthesis of sensing materials

In order to prepare the electrospinning solution, 400 mg of camphorsulfonic acid was added to 400 mg of polyaniline emeraldine base in a glass vial and 10 mL of chloroform was added to the mixture. In the second vial, 8.5 mL of chloroform and 1.5 mL of THF were added to the same amount of PAni and HCSA. The two vials were kept at room temperature under magnetic stirring (at 1500 rpm) for at least 12 hours. After dissolving the materials in the solvents by magnetic stirring, they were filtered by a PTFE hydrophobic syringe filter (pore size = 0.45 μm) in order to obtain a uniform solution for the electrospinning process. Also, a portion of filtered and unfiltered solutions were collected for UV-Vis spectroscopy. Then 3 wt% PEO was added to each solution and they were stirred for 4 hours. The solutions were filled in a glass syringe and electrospinning was carried out with the following parameters: the applied voltage was 10 kV, the pumping flow rate was 1 mL h^{-1}, and the grounded conductive substrate with a diameter of 90 mm was used with a rotation speed of 1000 rpm. The distance between needle tip and substrate was 6 cm. The electrospinning setup while running and the sensors immediately after the electrospinning are shown in Fig. 10(f) and (g), respectively. After the electrospinning, the sensors were collected and kept under nitrogen purging gas flow for 5 hours for the evaporation of the remaining solvent.

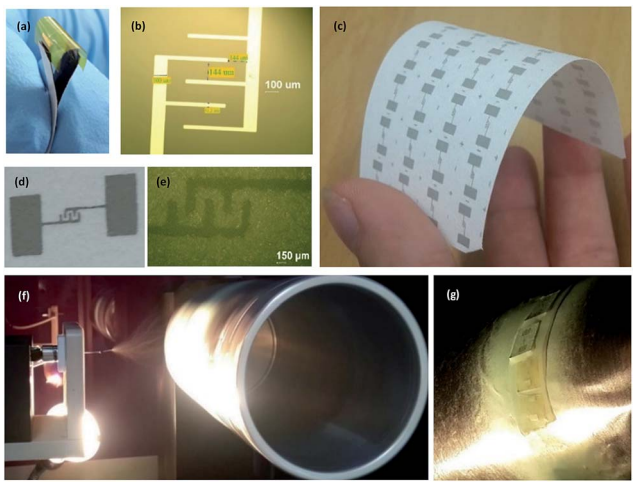

Fig. 10 (a) and (b) Polyimide sensor platform: gold interdigitated electrodes (100 nm thick) on PI film (15 μm thick); (c)–(e) paper sensor platform: screen printed carbon electrodes on paper; (f) fluid ejected from the needle's tip during electrospinning and (g) nanofibers deposited on the sensor substrates immediately after electrospinning.

Gas sensing setup

The sensors were tested in an enclosed chamber with a precise control of the flow rate and concentration of the gases. A source meter (Keithley 2636B) was used as the constant voltage source ($V_{DC} = 2$ volts) and also as the data acquisition system (real time resistance and current measurement). Labview™ was used to program the process and save the measurement data. The total flow rate used in the experiments was 200 sccm and the applied voltage was 2 V. The output resistance and voltage were variable depending on the RH chosen for each experiment, but the resistance was in the range of 800 kΩ to 6.5 MΩ. The resistance of the sensing materials deposited on the interdigitated electrodes shown in Fig. 10(b)–(e) with 150 μm electrode gap, were measured using Keithly 2636B source meter and a semiconductor parameter analyser. Also, the power consumption of the sensors was 0.6–5 μW ($P = V^2/R$).

Conclusion

In summary, a room temperature, flexible and low cost gas sensor was proposed. Sensing performance of the sensor was tested towards three types of environmentally harmful gases, namely H_2S, NO_2 and acetone. Our sensor showed high selectivity towards H_2S. The proposed sensor exhibits good sensitivity and quick recovery toward H_2S gas. The key to good recovery and repeatability of our sensor is the formation of high quality nanofibers web on the electrode that provides high surface to volume ratio and facilitates fast adsorption and desorption of H_2S gas molecules on the surface. These nanofibers were directly written on the paper and polyimide substrates as cheap and flexible substrates by electrospinning method. The sensor shows good stability over time when it is kept away from humidity. The sensor shows almost identical response after 1000 bending cycles, which proves that our sensor is highly flexible and robust and thus can be used in wearable applications. According to our experiments for synthesizing high quality and continuous nanofibers, an ambient relative humidity between 50% and 30% is required. Gas sensing tests in different RH conditions have been done to explore the dependence of the sensor's response on the RH. The average power consumption of our sensors is around 3 μW, which is very small. This low power consumption is one of the most important advantages of polymeric room temperature sensors over metal oxide sensors. Overall, we can conclude that the proposed sensor is very promising for room temperature detection of H_2S gas and can be used in many applications in which detection of low concentrations of H_2S gas is necessary.

Acknowledgements

This research was supported by Nano Material Technology Development Program (2015M3A7B7045518) through the National Research Foundation of Korea (NRF) funded by the Ministry of Science, ICT & Future Planning; project titled "Development of Management Technology for HNS Accident" funded by the Ministry of Oceans and Fisheries, Korea; and

National Research Foundation of Korea (NRF) (Grant No. 2015R1A5A1037668) funded by the Korean Government (MSIP).

Notes and references

1 S. Virji, R. B. Kaner and B. H. Weiller, *ACS Symp. Ser.*, 2007, **980**, 101–116.
2 "Hydrogen Sulfide", Agency for Toxic Substances and Disease Registry, http://www.atsdr.cdc.gov/phs/phs.asp?id=387&tid=67.
3 U.S. Department of Labor, Occupational Safety & Health Administration, https://www.osha.gov/dts/chemicalsampling/data/CH_246800.html.
4 M. Li, D. Zhou, J. Zhao, Z. Zheng, J. He, L. Hu, Z. Xia, J. Tang and H. Liu, *Sens. Actuators, B*, 2015, **217**, 198–201.
5 Z. Li, Y. Huang, S. Zhang, W. Chen, Z. Kuang, D. Ao, W. Liu and Y. Fu, *J. Hazard. Mater.*, 2015, **300**, 167–174.
6 V. Kruefu, A. Wisitsoraat, A. Tuantranont and S. Phanichphant, *Sens. Actuators, B*, 2015, **215**, 630–636.
7 Q. Zhou, A. Sussman, J. Chang, J. Dong, A. Zettl and W. Mickelson, *Sens. Actuators, A*, 2015, **223**, 67–75.
8 H. Liu, M. Li, G. Shao, W. Zhang, W. Wang, H. Song, H. Cao, W. Ma and J. Tang, *Sens. Actuators, B*, 2015, **212**, 434–439.
9 J. Petruci and A. A. Cardoso, *Anal. Methods*, 2015, **7**, 2687–2692.
10 K. Toda, R. Furue and S. Hayami, *Anal. Chim. Acta*, 2015, **878**, 43–53.
11 C. H. Moon, M. Zhang, N. V. Myung and E. D. Haberer, *Nanotechnology*, 2014, **25**, 135205.
12 E. Zampetti, S. Pantalei, S. Scalese, A. Bearzotti, F. De Cesare, C. Spinella and A. Macagnano, *Biosens. Bioelectron.*, 2011, **26**, 2460–2465.
13 N. J. Pinto, I. Ramosa, R. Rojas, P. C. Wang and A. T. Johnson, *Sens. Actuators, B*, 2008, **129**, 621–627.
14 J. Sarfraz, P. Ihalainen, A. Määttänen, J. Peltonen and M. Lindén, *Thin Solid Films*, 2013, **534**, 621–628.
15 S. Cho, J. Lee, J. Jun, S. G. Kim and J. Jang, *Nanoscale*, 2014, **6**, 15181.
16 S. K. Pandey, K. Kim and K. Tang, *TrAC, Trends Anal. Chem.*, 2012, **32**, 87–99.
17 K. Crowley, A. Morrin, R. L. Shepherd, M. Panhuis, G. G. Wallace, M. R. Smyth and A. J. Killard, *IEEE Sens. J.*, 2010, **10**, 9.
18 S. Virji, J. Huang, R. B. Kaner and B. H. Weiller, *Nano Lett.*, 2004, **4**, 3.
19 S. H. Hosseini, S. H. Abdi Oskooei and A. A. Entezami, *Iran. Polym. J.*, 2005, **14**, 333–344.
20 J. Sarfraz, D. Tobjork, R. Osterbacka and M. Linden, *IEEE Sens. J.*, 2012, **12**, 1973–1978.
21 Z. Li and C. Wang, One-Dimensional Nanostructures, *Springer Briefs in Materials*, Springer publishing, 2013.
22 S. Chaudhari, Y. Sharma, P. S. Archana, R. Jose, S. Ramakrishna, S. Mhaisalkar and M. Srinivasan, *J. Appl. Polym. Sci.*, 2013, **129**, 1660–1668.
23 Chemical Physics group, Lund university, http://www.chemphys.lu.se/old/kfresearch/com-conjupol.html.
24 G. Korotcenkov, *Handbook of Gas Sensor Materials: Properties, Advantages and Shortcomings for Applications*, Springer Publishing, 2013, vol. 1.
25 Y. Wang, P. Ding, R. Hu, J. Zhang, X. Ma, Z. Luo and G. Li, *Sensors*, 2013, **13**(3), 3765–3775.
26 Occupational safety and health guidelines for acetone, The National Institute for Occupational Safety and Health (NIOSH), http://www.cdc.gov/niosh/docs/81-123/pdfs/0004.pdf.
27 Nitrogen dioxide, The National Institute for Occupational Safety and Health (NIOSH), http://www.cdc.gov/niosh/npg/npgd0454.html.

